

AD-A043 123

NAVAL RESEARCH LAB WASHINGTON D C
ENHANCED BACKSCATTER WITH A STRUCTURED LASER PULSE. (U)
JUL 77 B H RIPIN, F C YOUNG, J A STAMPER

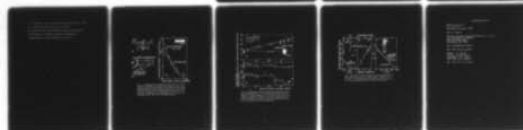
F/G 20/5

UNCLASSIFIED

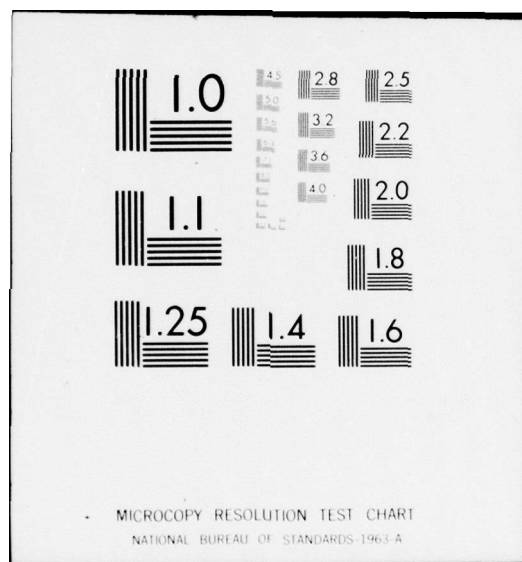
NRL-MR-3560

NL

1 OF 1
ADA043123



END
DATE
FILMED
9-77
DDC



AD A043123

12_{nu}

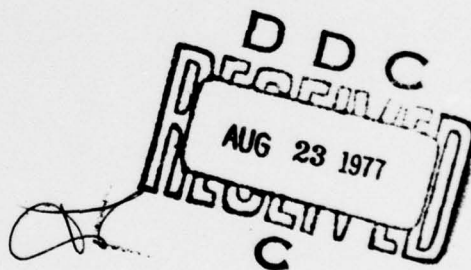
NRL Memorandum Report 3560

Enhanced Backscatter with a Structured Laser Pulse

B. H. RIPIN, F. C. YOUNG, J. A. STAMPER, C. M. ARMSTRONG,
R. DECOSTE, E. A. MCLEAN and S. E. BODNER

*Laser Plasma Branch
Plasma Physics Division*

July 1977



NAVAL RESEARCH LABORATORY
Washington, D.C.

Approved for public release: distribution unlimited.

AD No. _____
DDC FILE COPY

SECURITY CLASSIFICATION OF THIS PAGE (When Data Entered)

REPORT DOCUMENTATION PAGE		READ INSTRUCTIONS BEFORE COMPLETING FORM
1. REPORT NUMBER NRL Memorandum Report 3560 ✓	2. GOVT ACCESSION NO. (14)	3. RECIPIENT'S CATALOG NUMBER NRL-MR-3564
4. TITLE (and Subtitle) ENHANCED BACKSCATTER WITH A STRUCTURED LASER PULSE	5. TYPE OF REPORT & PERIOD COVERED	
7. AUTHOR(s) B.H. Ripin, F.C. Young, J.A. Stamper, C.M. Armstrong†, R. Decoste†, E.A. McLean and S.E. Bodner	6. PERFORMING ORG. REPORT NUMBER	
9. PERFORMING ORGANIZATION NAME AND ADDRESS Naval Research Laboratory Washington, D.C. 20375	8. CONTRACT OR GRANT NUMBER(s)	
11. CONTROLLING OFFICE NAME AND ADDRESS Energy Research and Development Administration Washington, D.C. 20545	10. PROGRAM ELEMENT PROJECT, TASK AREA & WORK UNIT NUMBERS NRL Problem H02-29A	
14. MONITORING AGENCY NAME & ADDRESS (if different from Controlling Office)	12. REPORT DATE July 1977	
	13. NUMBER OF PAGES 16	
	15. SECURITY CLASS. (of this report) UNCLASSIFIED	
	15a. DECLASSIFICATION/DOWNGRADING SCHEDULE	
16. DISTRIBUTION STATEMENT (of this Report) Approved for public release; distribution unlimited		
17. DISTRIBUTION STATEMENT (of the abstract entered in Block 20, if different from Report)		
18. SUPPLEMENTARY NOTES Work performed at the Naval Research Laboratory under the auspices of the U.S. Energy Research and Development Administration. *Supported by a NRC Associateship. †Supported by a Hydro-Quebec Fellowship at the University of Maryland.		
19. KEY WORDS (Continue on reverse side if necessary and identify by block number) Laser fusion Backscatter Absorption Structured pulse Brillouin backscatter		
20. ABSTRACT (Continue on reverse side if necessary and identify by block number) A large amplitude backscatter instability, consistent with Brillouin, occurs when a prepulse plasma is formed ahead of a high irradiance (10^{15} - 10^{16} W cm ²) Nd-laser pulse. These results indicate that temporally structured laser pulses suggested for laser pellet implosion may also encounter large backscatter.		

DD FORM 1473

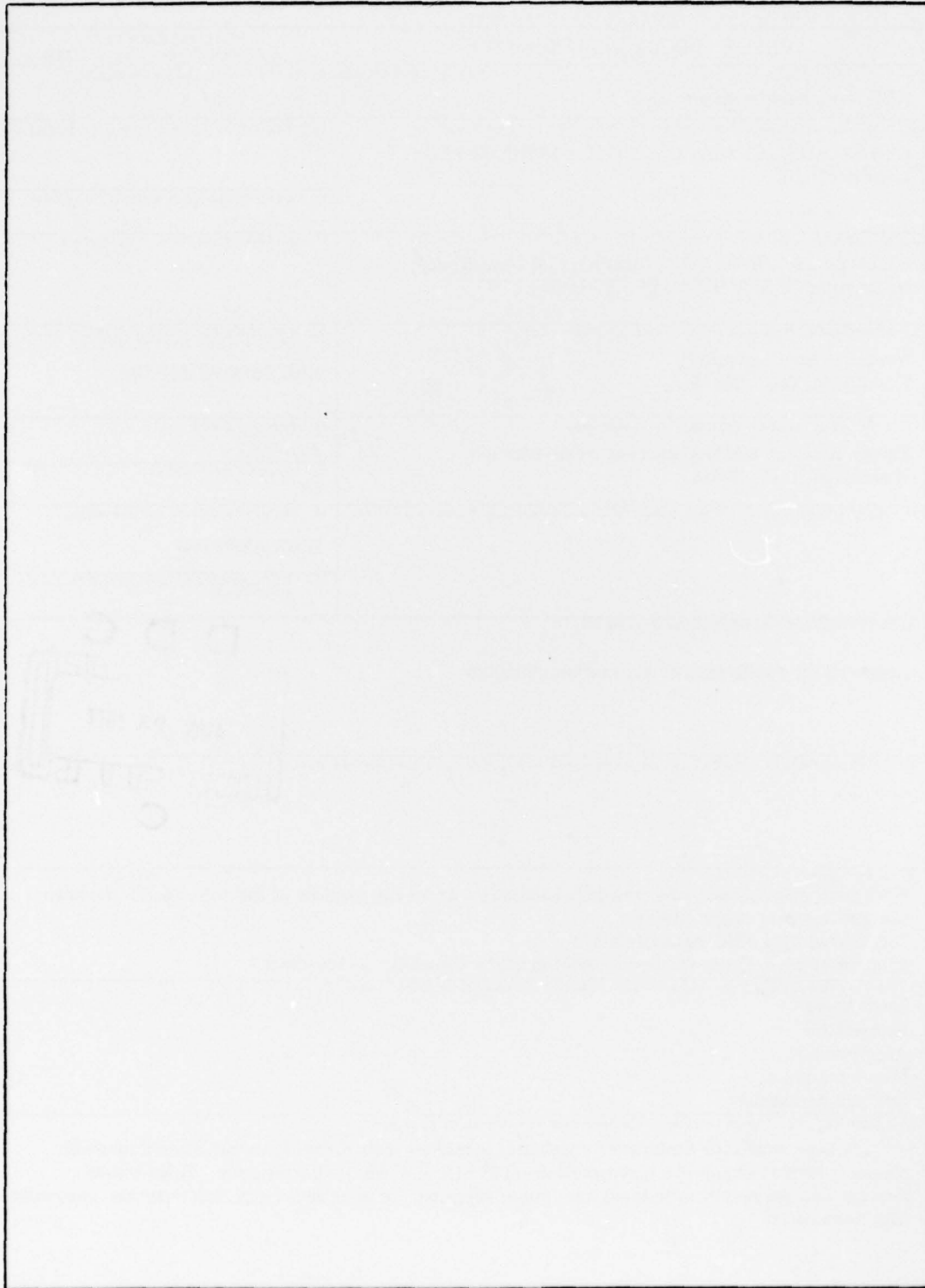
1 JAN 73

EDITION OF 1 NOV 65 IS OBSOLETE
S/N 0102-014-6601

SECURITY CLASSIFICATION OF THIS PAGE (When Data Entered)

251 950

SECURITY CLASSIFICATION OF THIS PAGE (When Data Entered)





ENHANCED BACKSCATTER WITH A STRUCTURED LASER PULSE

Precise laser pulse temporal shaping and good laser light absorption are usually required for successful implosion of laser-fusion pellets¹. In the experiments reported here we simulate the effect of a shaped pulse by first forming a plasma blowoff with a prepulse and then irradiating this preformed plasma with a short high-irradiance main pulse. The low density plasma resulting from the prepulse is likely to be similar to that produced by the long leading portion of some currently planned shaped pulses. Measurements show greatly enhanced direct backscatter² (by up to a factor of 3) and significantly reduced absorption of the second (main) pulse (in some cases to about 20%) in the presence of a prepulse-formed plasma. This backscatter appears to originate in the underdense region of the plasma ($n \leq 0.1 n_c$) and exhibits many of the properties of the Brillouin backscatter instability^{3,4}. No saturation of the backscatter instability appears in the energy range of this experiment. These results suggest that many of the shaped pulses proposed for laser fusion may have very poor coupling to the target plasma. The behavior of scattered light, x-rays, high energy ions and electrons, harmonic emission and density profile were obtained as functions of the prepulse level, the angle of irradiation of a planar target and the incident laser intensity.

Note: Manuscript submitted July 29, 1977.

One beam of the NRL Pharos II Nd-laser operating at $1.06 \mu\text{m}$, 75 psec pulse duration (FWHM) was focused with a $f/1.9$ aspheric lens onto the surface of polished planar polystyrene (CH) targets in an evacuated chamber. A controlled prepulse was introduced into the beam with the beam splitting arrangement shown in Fig. 1a. The relative timing of the prepulse to the main pulse was set at 2 nsec and the relative amplitudes were varied with attenuators A_p and A_m . Any unintentional prepulses were suppressed to below 10^{-7} of the total pulse energy by two saturable absorber cells and one Pockels cell in the laser chain. Three prepulse monitors were used on each shot to measure values of the ratio of the prepulse to main pulse ranging from 10^{-8} to 1. The half-energy content focal diameter was determined to be $30 \mu\text{m}$ by the multiple-image thin film ablation method⁵ yielding average and peak irradiances (for 9 J incident) of 7.5×10^{15} and $1 \times 10^{17} \text{ W/cm}^2$ respectively at normal incidence. A focal shift monitor was used to ensure on most shots that the target was in focus⁶.

Diagnostics operating on these experiments included incident and backreflection calorimeters, and an array of 18 minicalorimeters, all calibrated to $\pm 5\%$ accuracy (see Fig. 1b). On each shot the calorimeter array measured the angular distributions of scattered laser light both within (\parallel) and normal to (\perp) the plane containing the electric vector and wave vector of the incident laser beam. Also, fifteen filtered detectors for continuum x-rays from 1 to 600 keV, a magnetic electron spectrometer (50-500 keV), an ion charge collector (10-150 keV H^+), and a silicon photo-diode and spectrograph for monitoring laser harmonic

emission ($n \leq 5$) were employed. Interferometry of the prepulse-formed plasma at the arrival time of the second pulse was accomplished using a Raman shifted second-harmonic probe beam ($\lambda = 6329 \text{ \AA}$, time duration $\approx 35 \text{ psec}$) to obtain underdense plasma scale lengths and to ensure that single pulse cases had no prepulse plasma. The electron, ion and x-ray detectors, the harmonic emission and the interferometer were all viewing the plasma approximately midway between the \parallel and \perp planes of polarization of the incident laser beam. All detectors were near 45° to the target normal except for the four most energetic x-ray detectors and the interferometer which viewed the plasma tangent to the target surface at normal incidence.

An example of the effect of a prepulse upon the scattered light angular distribution, and therefore absorption efficiency, is shown in Fig. 1c. When a prepulse plasma is present, a dramatic increase of backreflection is seen compared to that measured without initial plasma at the target surface. The absorption decreases from about 50% without prepulse to 20% with the prepulse. The change in the angular distribution at angles outside the solid angle of the lens is not dramatically affected except possibly near 90° (which does not represent a large fraction of the scattered energy).

The dependence of the backscattered energy of the main pulse upon the prepulse-to-total-energy ratio, η , is shown in Fig. 2a for incident energies in the range of 7 to 11 J. For $\eta \geq 10^{-4}$ a significant, and monotonically increasing backscatter (to over 40%) is observed over that for a single pulse irradiation⁷. These data exhibited excellent

reproducibility when η was varied at random from shot-to-shot over the course of many days. Shots were taken with the prepulse alone (second pulse blocked) to ensure that the backreflection for a prepulse was the same as for a single pulse (they were) and to measure the prepulse energy directly as a check on the prepulse diode monitors. Included in Fig. 2a is a shot (*) for $\eta = 0.2$ where the laser was focused upon the prepulse plasma rather than on the target surface. Enhanced backscatter was observed under this condition as well.³

All other plasma emissions (x-rays, energetic ions and electrons, and harmonic emission) decreased with increasing prepulse level for $\eta > 10^{-3}$. Responses of two of the x-ray detectors (normalized to incident energy) are plotted as a function of prepulse level in Fig. 2b. A decrease in both x-ray intensity and hardness of the x-ray spectrum with increasing prepulse level is indicated. An obvious explanation for the decreased plasma emission with increasing prepulse level is the lowered irradiance and absorption in the critical and one-fourth critical regions of the plasma.

The enhanced backscatter occurring when the laser pulse irradiates a preformed plasma strongly suggests the action of a backscatter instability mechanism being operative.^{3,4} Measurements were made with the target rotated through various angles θ from normal incidence to test for the following two properties of Brillouin backscatter: First, a backscatter instability should cause the light to return through the focusing lens regardless of the target angle. Second, the incident laser light penetrates the plasma up to the turning point density n_t ,

below the critical density n_c , given in plane geometry by $n_t = n_c \cos^2 \alpha$. Thus, the target angle at which the enhanced backscatter effect drops off is indicative of the plasma density where the backscattering instability occurs. The results of backscatter measurements with and without a prepulse as a function of target angle are shown in Fig. 3a. With no prepulse the backreflection quickly drops off with angle as reported previously.⁹ However, with a $\eta = 0.2$ prepulse plasma the direct backscatter remains high even for target angles $> 75^\circ$, i.e., within 15° of grazing incidence! Here the stimulated backscatter is more than an order-of-magnitude larger than that for a single pulse. For $\alpha = 82^\circ$ it was verified that the reflected rays retrace the incident rays by blocking half the focusing lens and looking unsuccessfully for backscatter in the blocked half with burnpaper. Therefore, the density of the backscattering region is below $0.1 n_c$ assuming that the low density plasma is approximately one-dimensional.¹⁰ All of these properties; enhanced backscatter regardless of target angle, ray retracing and backscatter occurring in the underdense region are consistent with stimulated Brillouin backscatter. The nature of these properties of the large directed backscatter suggests that variations of target geometry (e.g., spherical) are not likely to alter this basic effect.

Figure 3b shows the incident energy dependence of the backscatter with an $\eta = 0.2$ prepulse. Enhanced backscatter is still present even though the beam energy is reduced by a factor of ten, i.e., to about 5×10^{14} W/cm² for the second pulse and there is no indication of

saturation of the instability with increasing energy.

Interferograms of the prepulse-formed plasma at the time of arrival of the main pulse, such as that shown in Fig. 3a, indicate the presence of long scale lengths in density ($\sim 100 \mu\text{m}$) below $0.1 n_c$ which are ideal for good growth of the Brillouin instability. The threshold for the Brillouin instability is well below all irradiances used here for the second pulse.

Brillouin backscatter convectively saturates with a net gain of $\exp(\lambda)$, with $\lambda = 2\pi v_0^2 / (cc_s dK/dx)$, where v_0 is the homogeneous growth rate, c_s is the ion acoustic velocity, and $K(x)$ is the wavenumber mismatch of the pump and scattered waves.³ Mismatch is usually ascribed to plasma density and velocity gradients. There is, however, another mismatch that is present even for a uniform plasma: the spatial gradients of the laser wave near the focus of a lens. This correlation length is usually referred to as the depth of focus. For example, a plane wave incident on a simple lens has on-axis distance between nulls of $4F^2\lambda_0$, where F is the f-number of the lens. For a laser or lens with aberrations, the correlation length (not the null distance) could be even less. (Away from focus, the correlation length will increase.)

There are thus two basic scale lengths: the light correlation length and the plasma density gradient. The role of the laser prepulse may be to increase the underdense plasma density scale length, and to increase the number of correlation lengths for the scatter, while the light

correlation length controls the mismatch. This may explain the relatively weak dependence of the scatter on prepulse energy. We do not yet have sufficient data to accurately determine the gain, $\exp(\lambda)$.

These experiments, which use a prepulse to simulate a temporally shaped pulse, strongly suggest that significant Brillouin backscatter may also occur in some currently planned shaped pulses. These shaped pulses generally deliver about one-half the total laser energy over many nanoseconds with a high-intensity (10^{15} - 10^{16} W/cm²) peak delivering the remaining energy in less than 1 nsec. The low density blowoff from such a temporally shaped pulse is likely to have a long scale length ideal for Brillouin backscatter of the high intensity peak such as found in our experiment. Because the density of the backscatter region appears to be low ($n \leq 0.1 n_c$) the ponderomotive force due to the final high intensity laser peak is not likely to steepen this gradient. Indeed, the presence of stimulated scatter in longer duration single pulse experiments is suggested by the fact that backscatter from 250 psec is greater than for 100 psec pulse for irradiances in the mid 10^{15} W/cm² range.⁵ Stimulated backscatter has also been observed in lower irradiance 900 psec pulse experiments both with and without a prepulse.⁴ It is obvious that experiments with the actual pulse shapes intended for laser fusion designs are needed to determine how severe a problem Brillouin backscatter will actually be

The larger surface area irradiations expected in these designs could tend to increase the backscatter over that observed here.

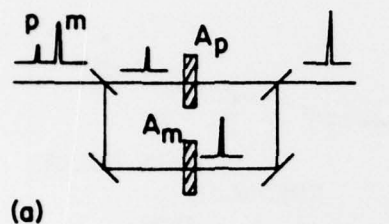
It is a pleasure to acknowledge the laser expertise of J. M. McMahon which made these experiments possible and R. W. Whitlock for aid during these experiments.

REFERENCES

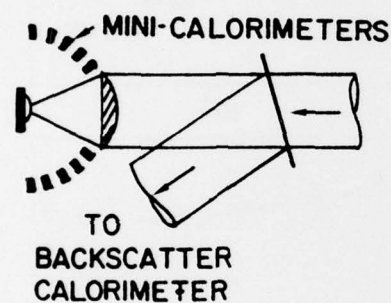
1. J. L. Nuckolls, L. Wood, A. Thiessen and G. Zimmerman, Nature 239, 139 (1972).
2. The term backscatter in this Letter refers only to the light scattered back into the solid angle of the focusing lens.
3. S. E. Bodner and J. L. Eddleman, Lawrence Livermore Laboratory Report 73378, 1971 (unpublished); C. S. Liu, M. N. Rosenbluth and R. B. White, Phys. Fluids 17, 1211 (1974); D. W. Forslund, J. M. Kindel and E. L. Lindman, Phys. Fluids 18, 1017 (1975); W. L. Kruer, E. J. Valeo and K. G. Estabrook, Phys. Rev. Lett. 35, 1076 (1975).
4. B. H. Ripin, J. M. McMahon, E. A. McLean, W. M. Manheimer and J. A. Stamper, Phys. Rev. Lett. 33, 634 (1974); L. M. Goldman, J. Soures and M. J. Lubin, Phys. Rev. Lett. 31, 1184 (1973).
5. B. H. Ripin, NRL Memo Report 3315, 1976 (unpublished).
6. J. A. Stamper, Appl. Optics 51, 2020 (1976).
7. A much smaller effect upon backreflection for prepulses with $\eta \geq 10^{-4}$ ($4\lambda > R > 1\lambda$) was noted previously by A. A. Gorokhov, V. D. Dyatlov, V. B. Ivanov, R. N. Medvedev and A. D. Starikov, JETP Lett. 21, 28 (1975). See also Ref. 4.
8. A 20% increase in scattered laser light for single pulse irradiation has been observed when the target is moved out of the focal region of the lens although no irradiance dependence was noted between 5×10^{14} and 10^{16} W/cm². B. H. Ripin, Proc. of 1977 IEEE Conf. on Plasma Science, pg. 66 (1977); and to be published. See also

C. G. VanKessel, et al., Max Planck Inst. Report IF IV/94 (1976).

9. B. H. Ripin, Appl. Phys. Lett. 30, 134 (1977).
10. The possibility that the plasma blow off may not be strictly one-dimensional for grazing incidence is suggested by interferograms at normal incidence such as Fig. 3c.



(a)



(b)

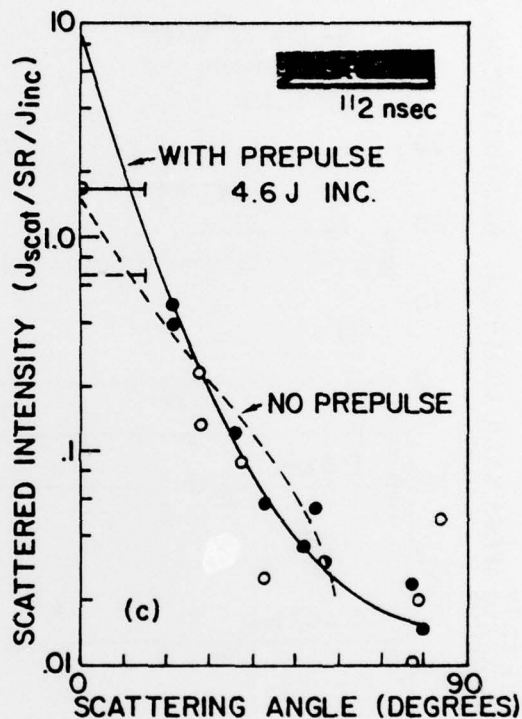


Fig. 1 — (a) Diagram of the optical path of the laser beams in the prepulse generator. (b) Diagram of the scattered light calorimeter layout. (c) Angular distributions of all scattered light for a typical single-pulse shot (dashed line) and a shot with a prepulse (solid line, (●) \perp -plane, (○) \parallel -plane). Horizontal bars between 0-15° are the backreflections averaged over the lens solid angle. Backreflection and total absorption are (15%, 50%) for the single pulse and (45%, 20%) for the double pulse respectively.

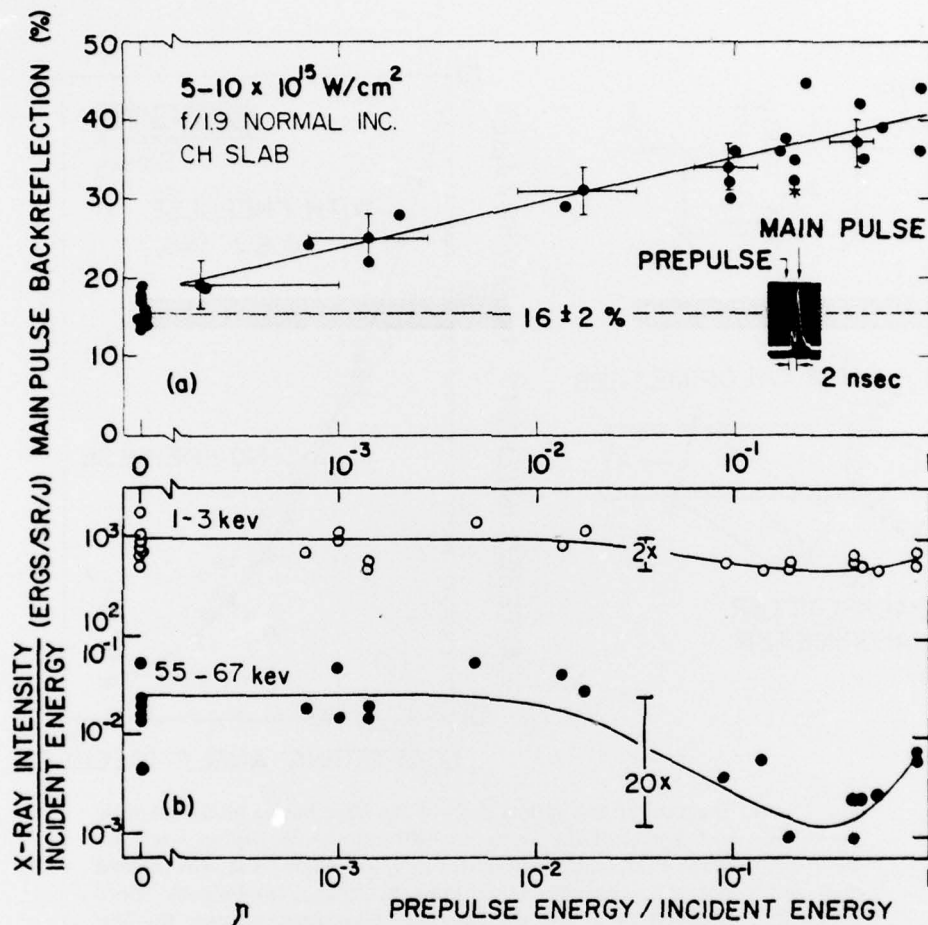


Fig. 2 - (a) Backreflections of the main pulse versus prepulse level showing enhanced backscatter for $\eta \gtrsim 10^{-4}$. Hashed region is the single pulse back-reflection. (b) X-ray intensities for 1-3 keV and 55-67 keV x-rays versus prepulse level illustrating the decrease in intensity and spectral hardness of x-rays with increasing η . (Increase in intensity for η approaching unity is due to x-ray emission induced by the prepulse itself.)

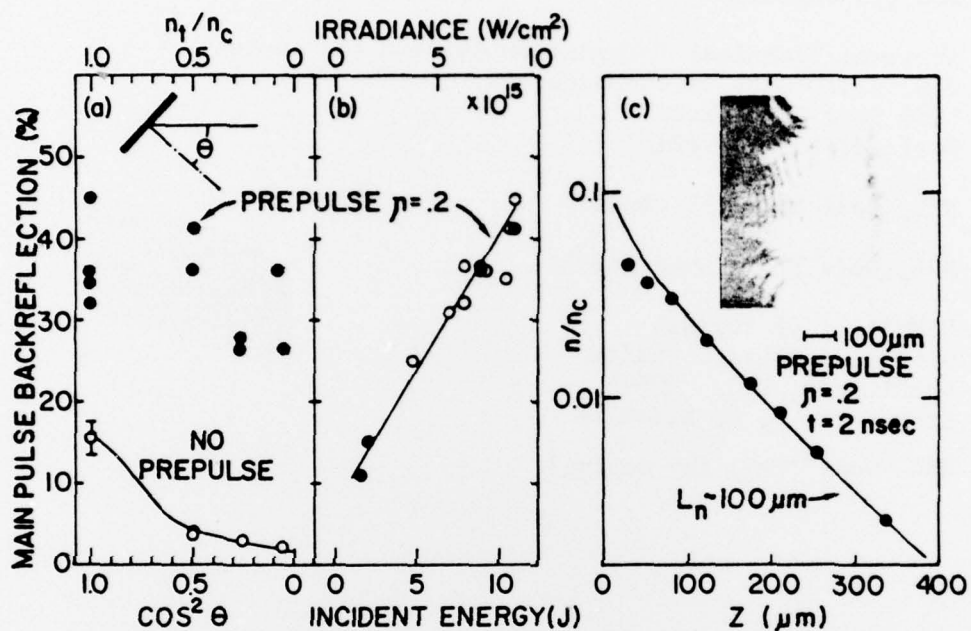


Fig. 3 — Backreflections of the main laser pulse versus (a) target angle θ (or turning point density), and (b) the incident energy or irradiance ((o) $\theta = 0^\circ$, (•) $\theta = 45^\circ$). (c) Interferogram and Abel inverted axial electron density profile of the prepulse plasma at the time of arrival of the main pulse.

DISTRIBUTION LIST

USERDA (50 copies)
P. O. Box 62
Oak Ridge, Tennessee 37830

DDC (12 copies)

National Technical Information Service (24 copies)
U.S. Department of Commerce
5285 Port Royal Road
Springfield, VA 22161

NRL, Code 2628 (35 copies)

NRL, Code 7730 (100 copies)

USERDA (3 copies)
Division of Laser Fusion
Washington, D.C. 20545
Attn: Dr. C. M. Stickley

NRL Code 7700, (25 copies)